Journal of Physics: Conference Series **202** (2010) 012008 doi:10.1088/1742-6596/202/1/012008

Network calculations for r-process nucleosynthesis

I Petermann[1,2], G Martínez-Pinedo[1], A Arcones[2,1], W R Hix[3], A Kelić[1], K Langanke[1,2], I Panov[6], T Rauscher[4], K-H Schmidt[1], F-K Thielemann[4], N Zinner[5]

[1] GSI Helmholtzzentrum für Schwerionenforschung, Darmstadt, Germany
[2] Institut für Kernphysik, TU Darmstadt, Germany
[3] Physics Division, Oak Ridge National Laboratory, Oak Ridge, TN37831-6374, USA
[4] Department für Physik und Astronomie, Universität Basel, Switzerland
[5] Department of Physics, Harvard University, Cambridge, MA 02138
[6] Institute for Theor. and Exp. Physics, B Cheremushkinskaya St 25, 117218 Moscow, Russia

Abstract. The r-process is known to be responsible for the synthesis of about half of the elements heavier than iron, nevertheless its astrophysical site has not yet been clearly ascertained, but observations indicate that at least two possible sites should contribute to the solar system abundance of r-process elements. The r-process being responsible for the production of elements heavier than $Z = 56$ operates rather robustly always resulting in a similar relative abundance pattern. From the nuclear-physics point of view the r-process requires the knowledge of a large number of reaction rates involving exotic nuclei that are not accessible by experiment and data have to be provided by theoretical predictions. We have developed for the first time a complete database of reaction rates that in addition to neutron-capture rates and β-decay half-lives includes the dominant reactions that can induce fission (neutron-capture, β-decay and spontaneous fission) and the corresponding fission yields. In addition, we have implemented these reaction rates in a fully implicit reaction network. The influence of the nuclear physics input constituted in the reaction rates based on the two mass models FRDM and ETFSI and on the astrophysical conditions simulating a cold or hot environment are examined.

1. Introduction

The r-process is a series of rapid neutron-capture reactions and β-decays in explosive scenarios with high neutron densities. Its astrophysical site remains uncertain, but observations indicate the contribution of at least two sites, namely core collapse supernovae from stars of different masses and neutron-star mergers. Observed abundances of r-process elements with $Z > 56$ in metal-poor stars follow a very robust pattern, that is consistent with scaled solar abundances[1]. Our aim is to explore whether or not fission can provide an explanation for the robustness.

2. Fission in the r-process

R-process simulations require in addition to neutron captures and β-decays a full set of fission rates [2], supplemented by all corresponding fission yields. We have considered neutron-induced fission, computed using the SMOKER code [3], β-delayed fission and spontaneous fission. For all of them fission yields have been computed using the statistical code ABLA [4], taking the neutrons evaporated explicitly into account. The resulting rates have been implemented in a fully implicit network, that includes approximately 7000 nuclei from n, p up to ^{300}Ds. The set of differential equations is linearized and solved using the Newton-Raphson method [5]. The

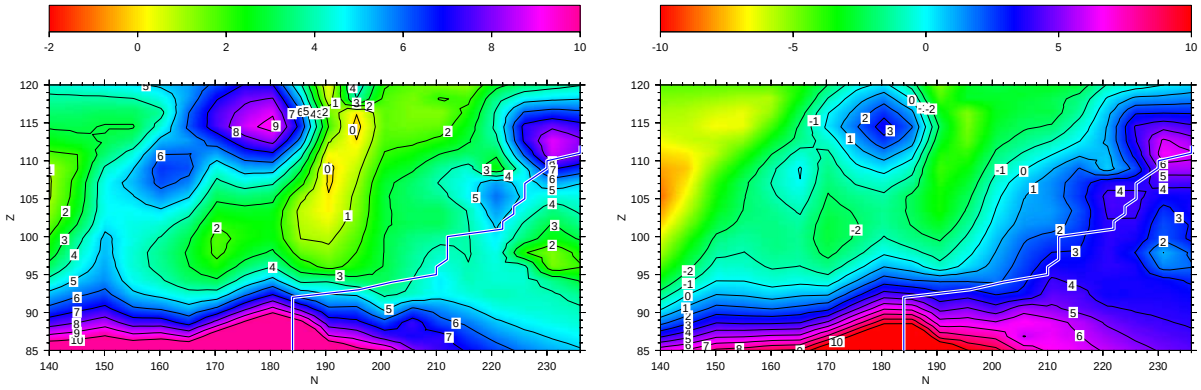

Figure 1. Region of the nuclear chart where fission takes place during the r-process. In the left panel the contour lines show the Myers-Swiatecki fission barrier heights (B_f) in MeV. The right panel shows contour lines of the quantity $B_f - S_n$, with S_n the neutron separation energy taken from the FRDM mass model. The unlabeled line shows the location of the neutron dripline.

inclusion of fission maintains the sparseness of the matrix and allows to use sparse matrix solvers, in our case the Parallel Sparse Direct Linear Solver (PARDISO) was used [6].

Fig. 1 shows the region where fission takes place during the r-process for the combination of Myers-Swiatecki [7] fission barrier heights and the neutron separation energies based on the FRDM mass model. Once the matter-flow breaks out of the magic neutron number $N = 184$ the fission barriers decrease drastically, and fission becomes possible.

3. Network calculations

We have performed network calculations using trajectories obtained from model M15-l1-r1 from the hydrodynamical simulations of ref. [8]. By increasing the entropy obtained in these simulations, large enough neutron-to-seed ratios could be achieved for a successful r-process.

Besides the total fission rate it is also instructive to specify the dominating fission channel. Fig. 2 shows the evolution of the fission rates for the different channels. They are computed determining the instantaneous increase in the total abundance of r-process nuclei, having $A \geq 5$, due to each fission channel. Clearly neutron induced fission is the dominating channel with β-delayed fission having a slight influence. The end of the r-process can be seen around 1.3 s by the sudden drop in the neutron-to-seed ratio. This is followed by a phase where all heavy fissioning nuclei decay over a timescale of several hundreds of seconds. During this phase neutron induced fission still dominates due to the neutrons produced by fission.

For an examination of the possible build-up of superheavy elements a comparison of the largest rates including β-delayed fission, spontaneous fission, alpha and β^- decay for FRDM with Myers-Swiatecki barriers and ETFSI masses and barriers [9] is shown in Fig.3. For FRDM an impassable barrier made up by spontaneous fission rates prevents a progressive motion of the nucleosynthesis front towards (super)heavy elements. For the case of the ETFSI mass model the area of spontaneous fission constituting the largest rate shows a clear split with a small passage permitting to reach heavier elements.

The lowermost point in the N-Z-plane constitutes the last element that can via β-decay contribute to a build-up of heavier elements while nuclei beyond that point will immediately decay via spontaneous fission in lighter fragments that are not available for an augmentation of heavy elements. This point lies at higher proton and neutron numbers for the ETFSI mass model, which can serve as a possible explanation for the observation of a slightly larger amount of heavy elements in this mass model compared to FRDM as shown in Fig. 4 in a direct comparison

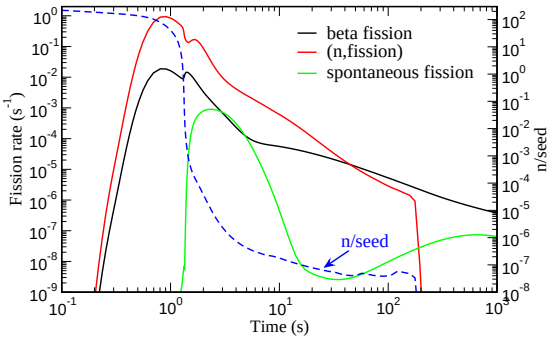

Figure 2. Evolution of the fission rate for the different channels for a calculation with initial neutron-to-seed ratio 295. Time zero corresponds to the beginning of the r-process phase after alpha-rich freeze-out. The evolution of the neutron-to-seed ratio is also shown (dashed line).

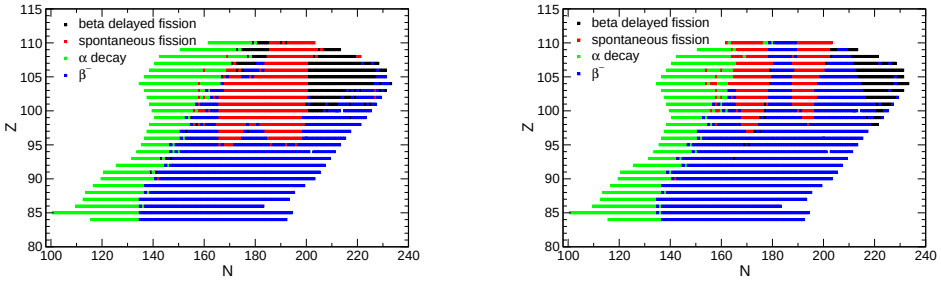

Figure 3. The largest rates for FRDM (left) and ETFSI (right).

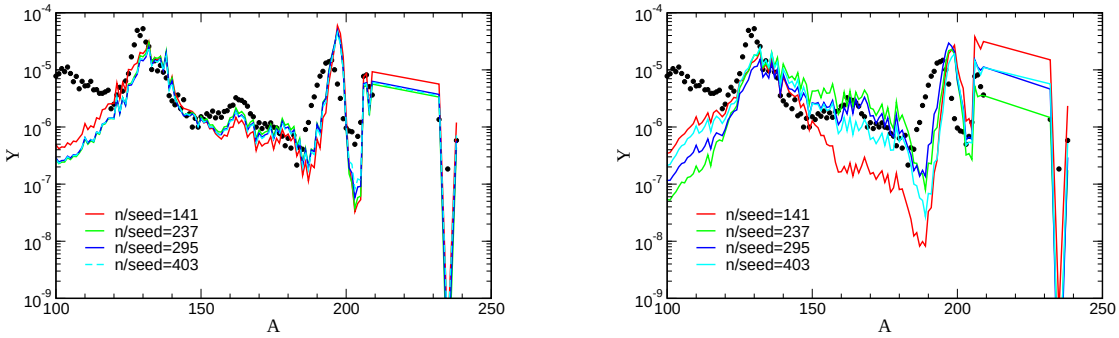

Figure 4. R-process abundances after a time of 13 Gy resulting from four calculations with different initial neutron-to-seed ratios for the two mass models FRDM and ETFSI. The black dots show the r-process solar distribution.

of the abundances at a time obtained after a time of 13 Gy, in each case for four initial neutron-to-seed ratios. In addition only small differences comparing the four abundance curves in the case of FRDM are existent, while the convergence behaviour in the case of ETFSI is observable, but much less distinct. In the case of a neutron-to-seed ratio of 141 a clear divergence compared to the ones for n/seed=237, 295 can be seen. Besides the impact of the nuclear physics input an analysis of the effect of the astrophysical conditions on the final abundance pattern was made. Therefor calculations were performed in a low-temperature environment, where the neutron emission by photodisintegration is insignificant and in a hot environment, where an (n,γ)-(γ,n) equilibrium is maintained for an essential period of time. Starting with an initial neutron-to-seed ratio of 295 a comparison for n/seed=100 and n/seed=1, constituting the termination

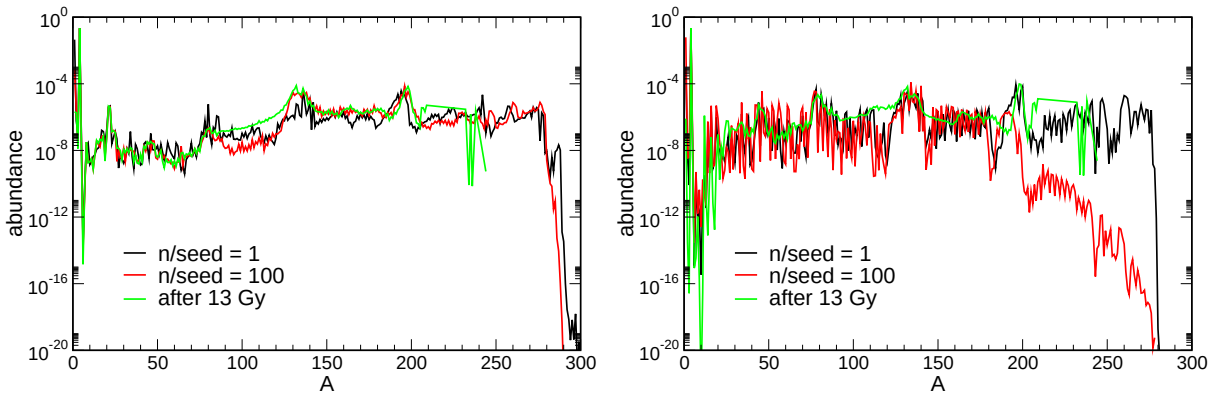

Figure 5. Abundances for neutron-to-seed ratios 100 and 1 for cold (left) and hot (right) astrophysical conditions with FRDM mass model and initial neutron-to-seed ratio 295.

point of the r-process, is shown for the two cases in Fig.5. For conditions of a cold r-process (left) the maximum massnumber A∼290 is already reached at early times (n/seed=100) allowing for a longer period of time where fission can take place supplementing nuclei in the medium-heavy massrange made available for an onward fission cycling process. This is in contrast to the case of a hot r-process where at a neutron-to-seed ratio of 100 a significant abundance is only existent up to a massnumber of A=200, compared to a an A(max) of 280. A pronounced pattern in the abundance distribution indicates the sensitivity to the underlying structure of the neutron-separation energies. Despite the distinct differences at intermediate timesteps the final abundance distribution at a time of 13 Gy is comparable, the peaks at A=130 and 195 are comparable well reproduced, nevertheless variations are seen in the smaller mass range.

4. Summary

The influence of fission in the r-process has been examined using a full set of reaction rates that include all possible fission channels, supplemented with the corresponding fission yield distributions. In our calculations neutron induced fission turned out to be the dominating channel, which is in agreement with results obtained in ref. [11] in studies of r-process in neutron star mergers. Furthermore, calculations with different initial neutron-to-seed ratios give very similar final abundance distributions for calculations based on the mass model FRDM, while a convergence is less obvious in the case using the ETFSI mass model. Trajectories simulating a cold or hot environment give comparable results in the final abundance pattern, while the strong influence of neutron separation energies is seen in the case of a hot r-process where the (n,γ)-(γ,n) equilibrium is maintained for a longer timescale.

References

[1] J. J. Cowan and C. Sneden, Nature **440**, 1151 (2006).
[2] J. J. Cowan, F.-K. Thielemann, J. W. Truran, Phys. Rep. **208** 267-394 (1991).
[3] I. Panov et al., Nucl.Phys. A **747**, 633-654 (2005). I. Panov, *et al.*, in preparation.
[4] J.-J. Gaimard and K.-H. Schmidt, Nucl. Phys. A **531**, 709 (1991).
[5] W. R. Hix, F.-K. Thielemann, Journal of Computational and Applied Mathematics **109**, 321-351 (1999).
[6] O. Schenk and K. Gärtner, Journal of Future Generation Computer Systems **20**, 475 (2004).
[7] W. D. Myers and W. J. Swiatecki, Phys. Rev. C **60**, 014606 (1999).
[8] A. Arcones, H.-Th. Janka, L. Scheck, A&A, **467**, 1227 (2007).
[9] A. Mamdouh, J. M. Pearson, M. Rayet, F. Tondeur, Nucl. Phys. A **644**, 389 (1998).
[10] P. Moller, J. R. Nix and W. J. Swiatecki, Atomic Data Nucl. Data Tables **59** 185 (1995).
[11] I. V. Panov and F.-K. Thielemann, Astronomy Letters **30**, 647 (2004).